Supporting Information

V_4C_3 MXene-derived $Zn_{0.99}V_5O_{12}\cdot nH_2O$ nanoribbons as advanced cathodes for ultra-long life aqueous zinc-ion batteries

Wenhai Xiao,[a] Shenghong Yang,[a] Rui Jiang,[a] Qiaofeng Huang,[a] Xiaoyan Shi,[a] Yuen Hong Tsang,[b] Lianyi Shao*[a] and Zhipeng Sun*[a]

[a.]School of Materials and Energy, Guangdong University of Technology, Guangzhou 510006, Guangdong, China. E-mail: shaolianyi@gdut.edu.cn, zpsunxj@gdut.edu.cn

[b.]Department of Applied Physics and Materials Research Center, The Hong Kong Polytechnic University, Hung Hom, Kowloon, Hong Kong, China.

Experimental Section

Material characterization

X-ray diffraction (XRD) patterns were collected by Rigaku SmartLab diffractometer with Cu Kα radiation. Raman patterns were collected by LabRAM HR Evolution. The microstructure morphologies of the as-synthesized products were performed by field emission scanning electron microscope (SEM, JEOL-6300F/Apreo 2S HiVac) and transmission electron microscope (TEM, Spectra 300, Thermo Fisher Scientific). The content of Zn^{2+}/Co^{2+}/Ni^{2+} was determined quantitatively by inductively coupled plasma mass spectrometry (ICP-MS, ICAP RQ, Thermo Fisher). The elemental distribution was obtained by energy dispersive spectroscopy (EDS, XFlash®6|60). Thermogravimetric analysis (TGA) was conducted by TGA 4000 in the air with a heating rate of 10 ℃ min^{-1}. X-ray photoelectron spectroscopy (XPS) was conducted on a Thermo Scientific K-Alpha spectrometer equipped with a monochromatic Al Kα X-ray source (1486.6 eV) operating at 100 W.

Electrochemical Characterization

The working electrodes were fabricated by mixing $Zn_{0.99}V_5O_{12}\cdot nH_2O$ with superconducting carbon black and polyvinylidene fluoride (PVDF) at a weight ratio of 7:2:1 in N-methyl-2-pyrrolidone (NMP). The obtained slurry was evenly coated on a 500 mesh stainless steel mesh and then vacuum dried at 60°C for 12 h. The active material in the electrode for the coin battery was 1.5-3 mg cm^{-2}. The mass of active material in the soft packaging battery was around 0.9-1.6 mg cm^{-2}. Using 3M $Zn(CF_3SO_3)_2$ aqueous solution as the electrolyte, glass fiber as a separator, and metal zinc as a negative electrode, the coin/soft packaging batteries were assembled in the air. The soft packaging batteries were assembled using aluminum-plastic film as the outer packaging. The air was pumped out by the heat-collecting vacuum sealing machine. The electrochemical performance of these batteries was tested using the Neware battery testing system (CT4008T) at 0.2-1.6 V. The electrochemical impedance spectroscopy and cyclic voltammetry curves were tested by the Chenhua Electrochemical Workstation (CHI760E).

The galvanostatic intermittent titration technique (GITT) was employed to measure the Zn^{2+} diffusion coefficient ($D_{Zn^{2+}}$) within a charge/discharge time of 10 mins and followed by a relaxation time of 30 mins at 0.1 A g^{-1}. The assembled ZIBs were first discharged and charged in two cycles at 0.1 A g^{-1} to reach a stable state. Then the GITT measurements were taken. $D_{Zn^{2+}}$ was calculated according to the following formula:

$$D_{Zn^{2+}} = \frac{4}{\pi\tau}\left(\frac{m_B V_M}{M_B S}\right)^2\left(\frac{\Delta E_s}{\Delta E_\tau}\right)^2$$

where m_B, M_B, and V_M refer to the mass loading (g), molar mass (g mol^{-1}), and molar volume (cm^{-3} mol^{-1}) for ZnVO, τ is current pulse time (s), ΔE_τ and ΔE_s represent the voltage variation (V) during the constant current pulse of one single-step GITT test after removing the IR drop and the steady-state potential change (V) by the current pulse during one single-step GITT process, respectively.[1]

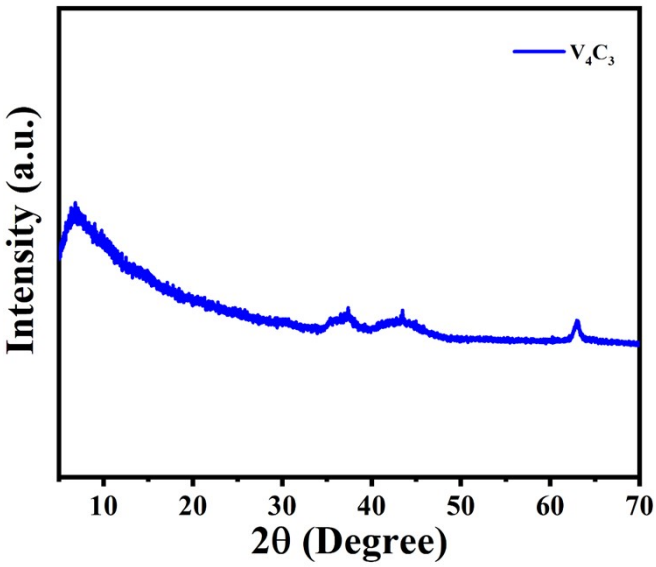

Fig. S1 XRD pattern of V_4C_3.

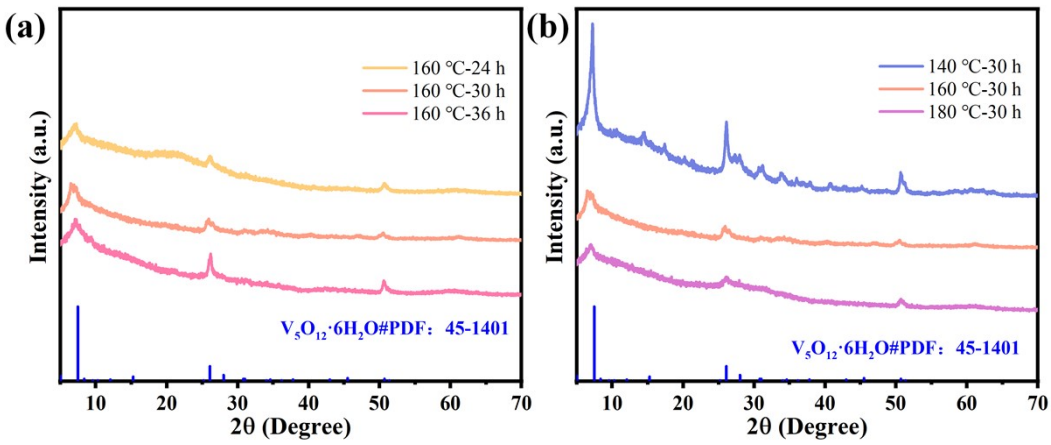

Fig. S2 XRD patterns of ZnVO synthesized at different a) times and b) temperatures.

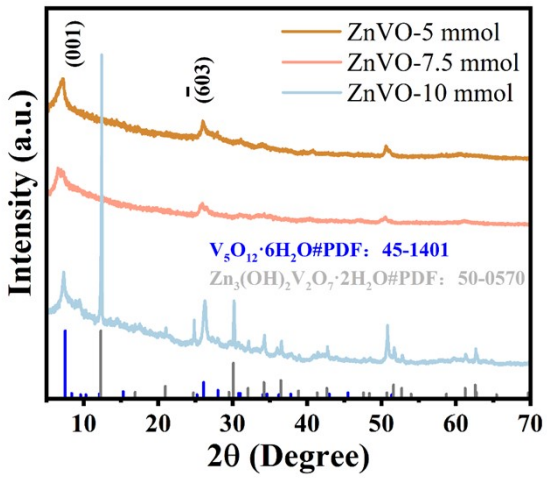

Fig. S3 XRD patterns of ZnVO synthesized at different Zn^{2+} concentration.

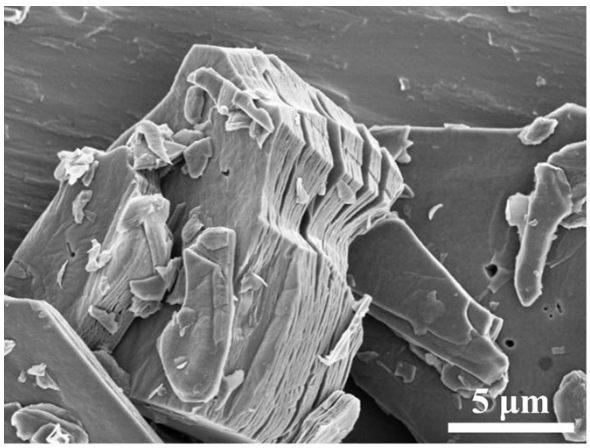

Fig. S4 SEM image of V_4C_3 raw material.

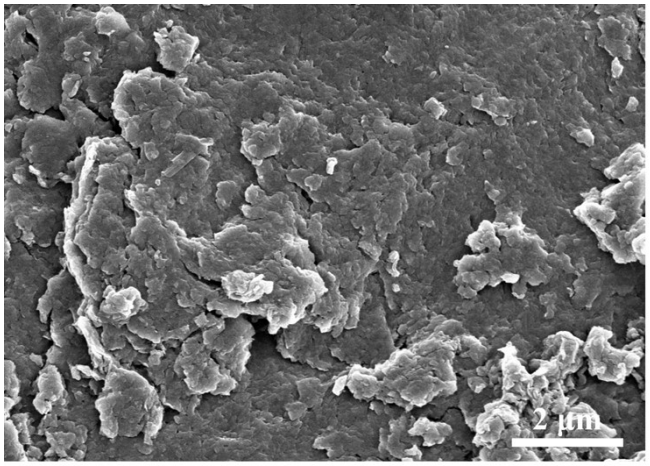

Fig. S5 SEM image of CoVO.

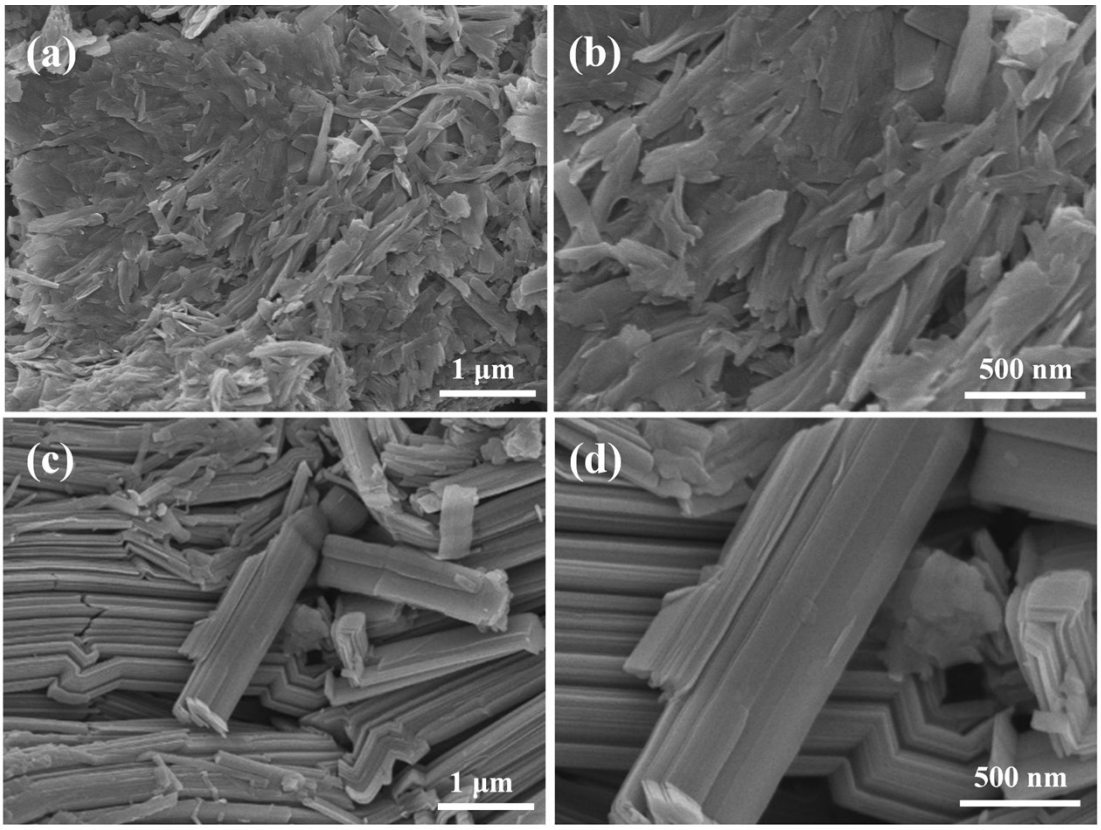

Fig. S6 SEM images of (a, b) ZnVO-160 °C-24 h and (c, d) ZnVO-160 °C-36 h.

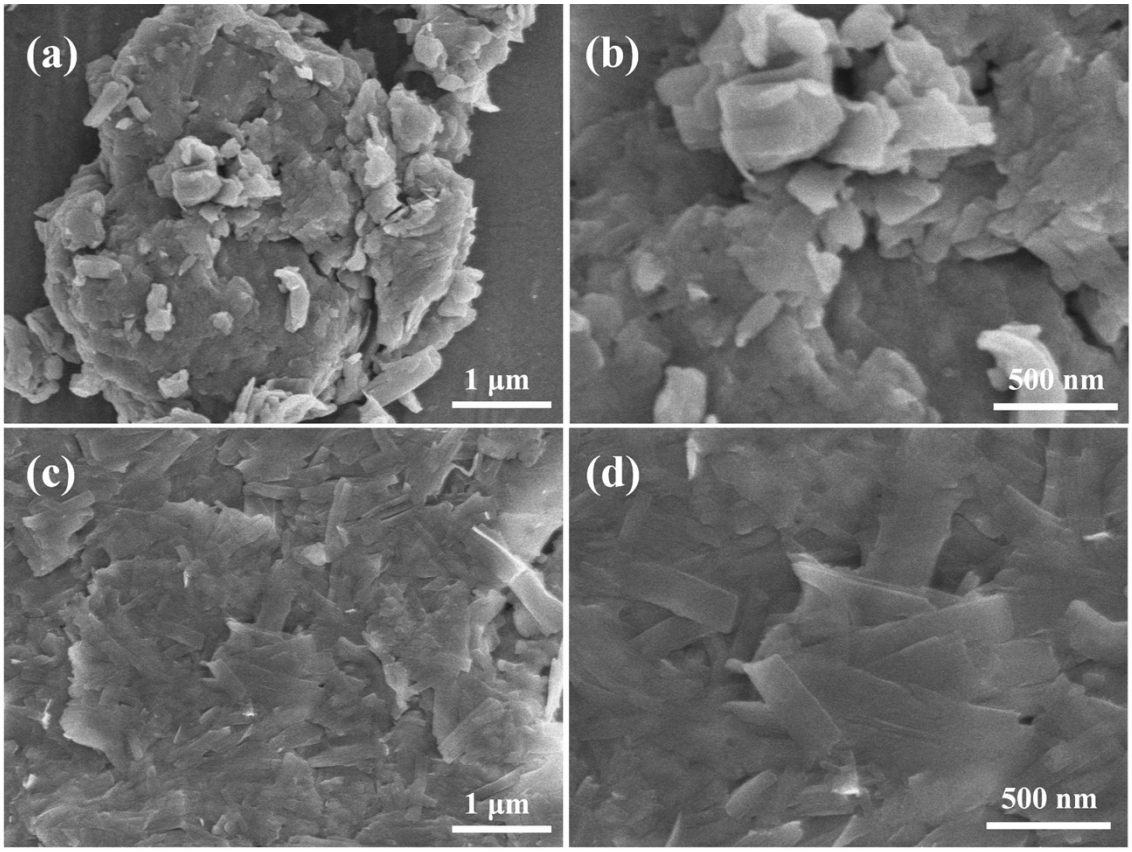

Fig. S7 SEM images of (a, b) ZnVO-140 °C-30 h and (c, d) ZnVO-180 °C-30 h.

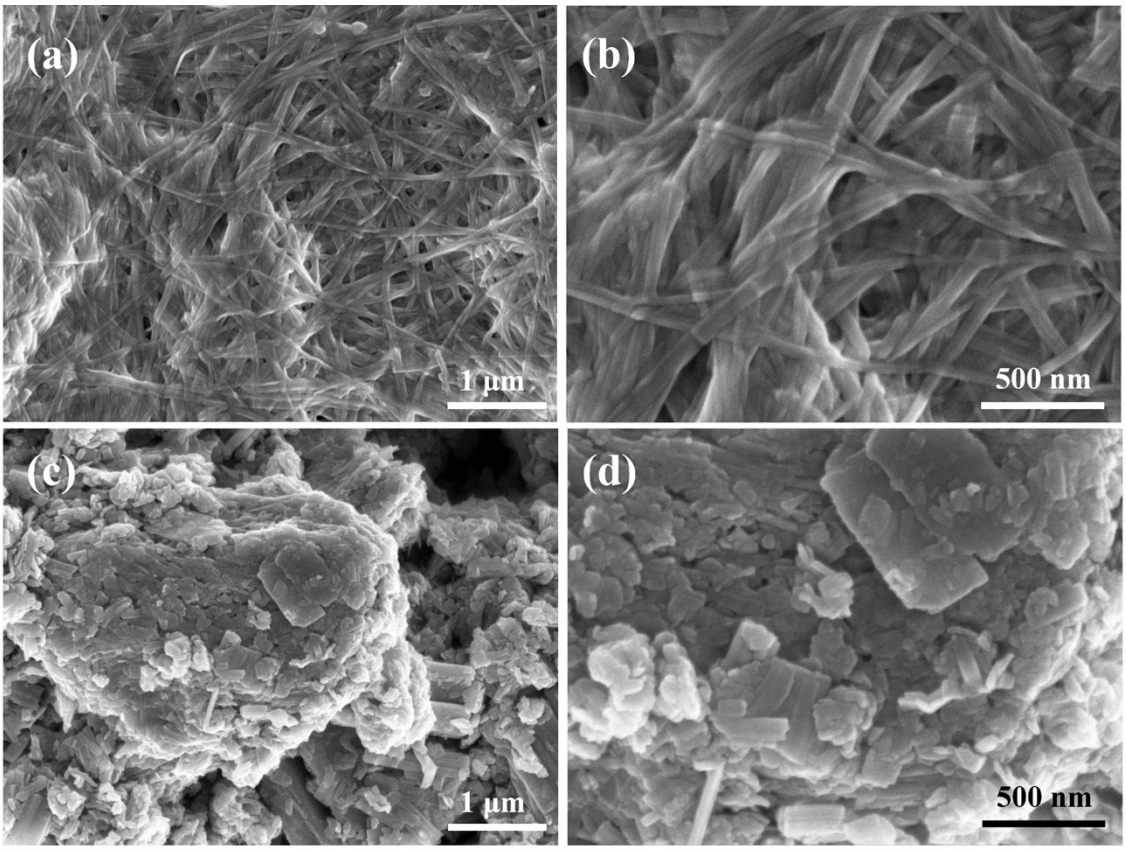

Fig. S8 SEM images of (a, b) ZnVO-160 °C-30 h-5 mmol and (c, d) ZnVO-160 °C-30 h-10 mmol.

(a)

Elt.	Line	Intensity (c/s)	Atomic %	Conc.	Units	Error 2-sig	MDL 3-sig	
O	Ka	42.85	68.962	40.001	wt.%	2.900	2.835	
V	Ka	121.87	25.929	47.886	wt.%	1.796	1.297	
Zn	Ka	5.79	5.109	12.113	wt.%	3.382	4.345	
			100.000	100.000	wt.%			Total

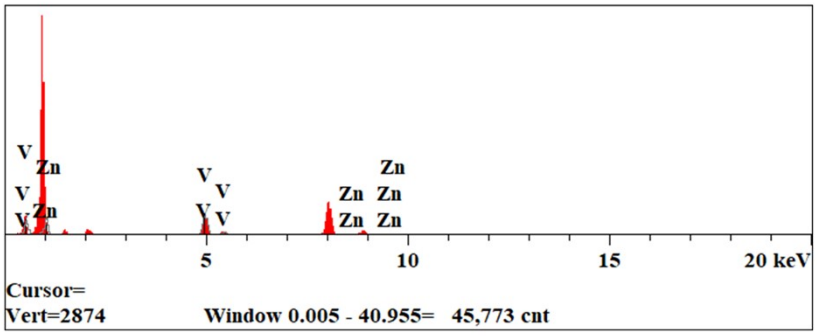

(b)

Elt.	Line	Intensity (c/s)	Atomic %	Conc.	Units	Error 2-sig	MDL 3-sig	
O	Ka	85.47	65.248	36.751	wt.%	1.582	0.963	
V	Ka	360.70	31.458	56.416	wt.%	1.128	0.475	
Co	Ka	18.93	3.294	6.833	wt.%	0.793	0.838	
			100.000	100.000	wt.%			Total

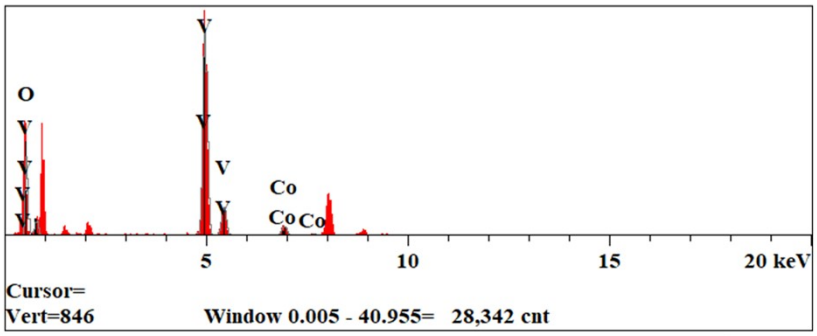

(c)

Elt.	Line	Normalized mass (%)	Atomic %	Abs. error (%)
O	Ka	34.86	63.41	1.47
V	Ka	56.90	32.50	1.87
Ni	Ka	8.24	4.08	0.37
		100.000	100.000	

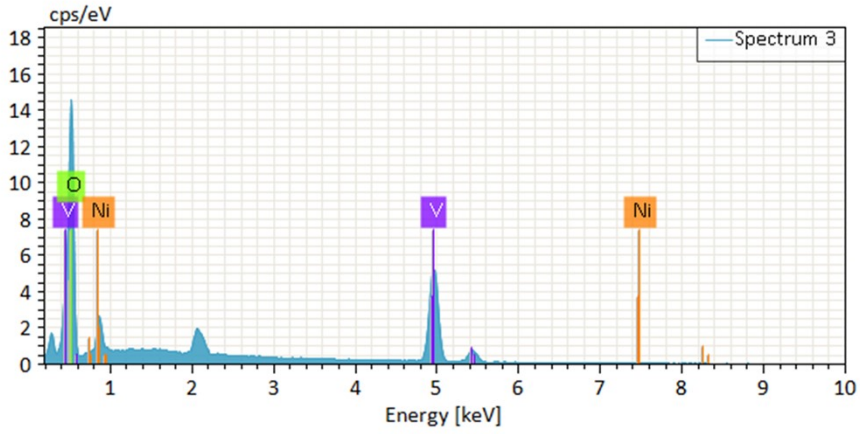

Fig. S9 EDS reports of a) ZnVO, b) CoVO, and c) NiVO.

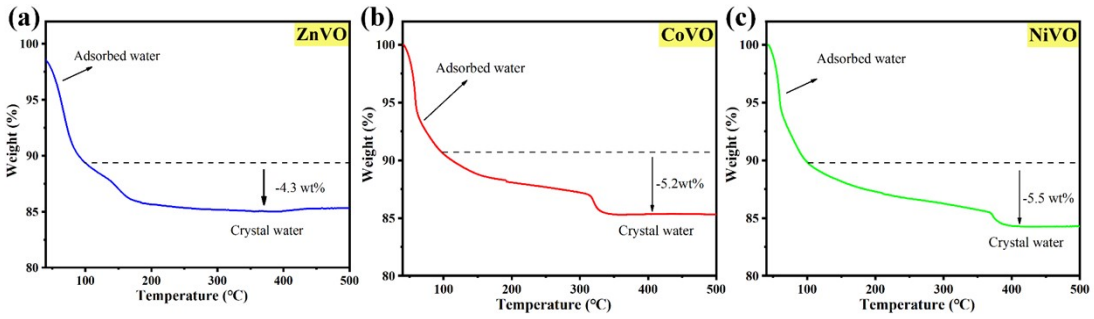

Fig. S10 TGA curves of a) $Zn_{0.99}V_5O_{12}\cdot nH_2O$, b) $Co_{0.60}V_5O_{12}\cdot nH_2O$, and c) $Ni_{0.58}V_5O_{12}\cdot nH_2O$.

The formula for calculating the content of crystal water is as follows:

$$m_a = \frac{18n}{M}$$

where m_a is the weight loss rate of crystalline water, n is the number of crystalline water, and M is the molar mass of the material.

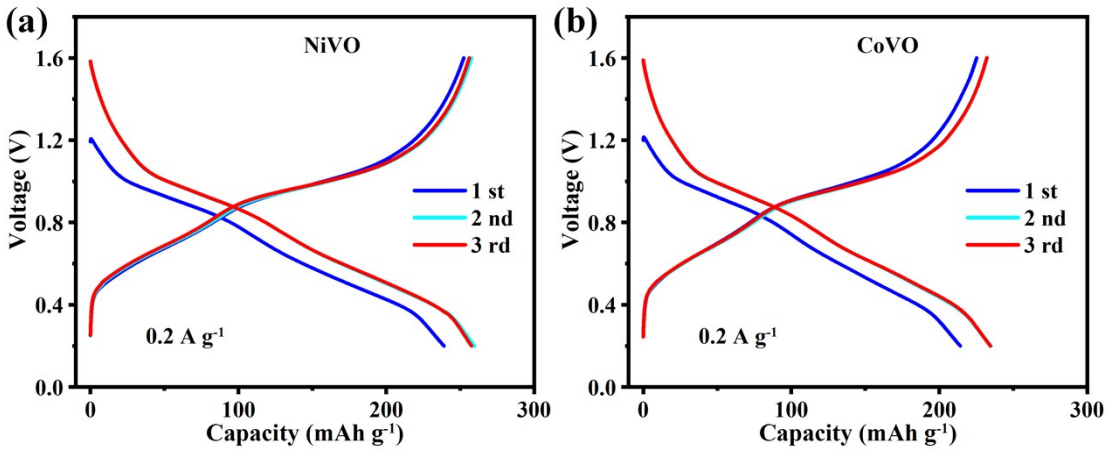

Fig. S11 The initial three charge-discharge curves of a) NiVO and b) CoVO at 0.2 A g^{-1}.

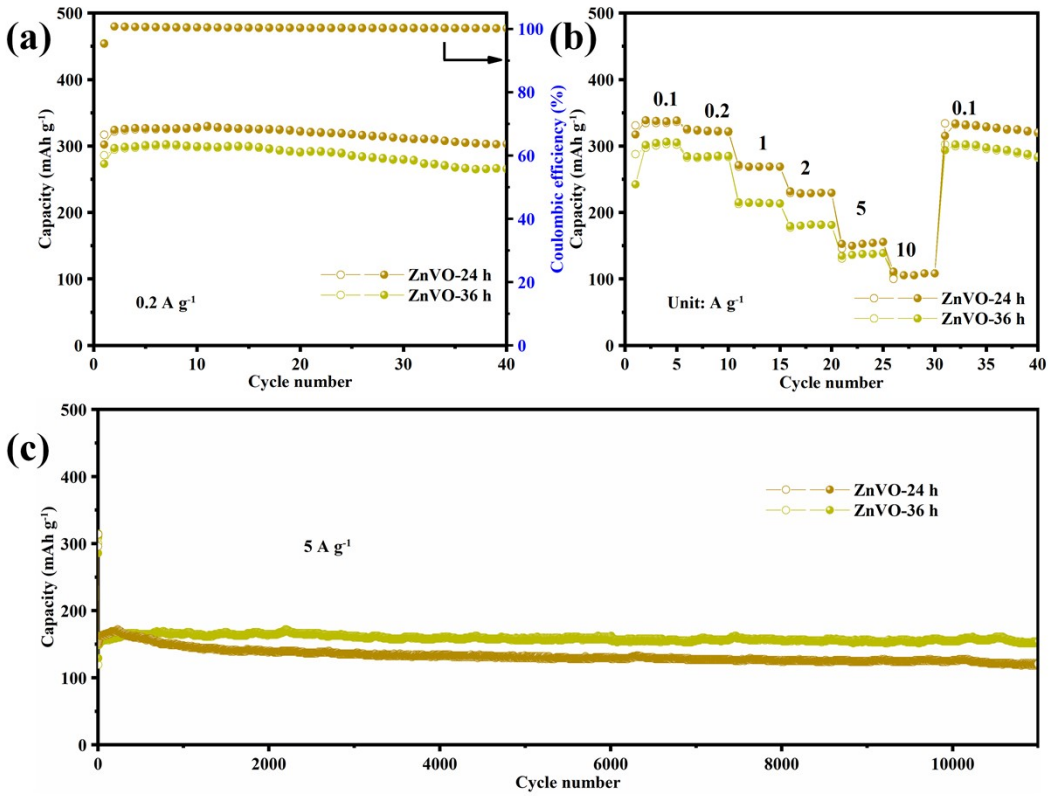

Fig. S12 a) Cycling performance at 0.2 A g^{-1}, b) rate performance, and c) long cycling performance at 5 A g^{-1} of ZnVO prepared at 160 ℃ for different times.

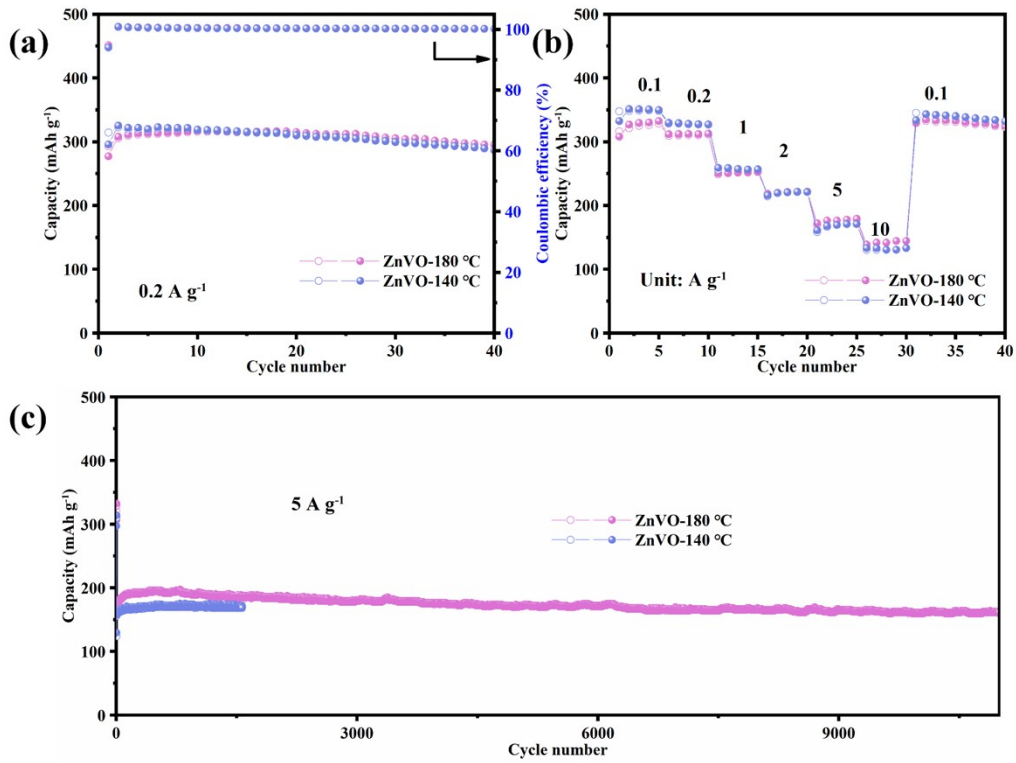

Fig. S13 a) Cycling performance at 0.2 A g^{-1}, b) rate performance, and c) long cycling performance at 5 A g^{-1} of ZnVO prepared at different temperatures.

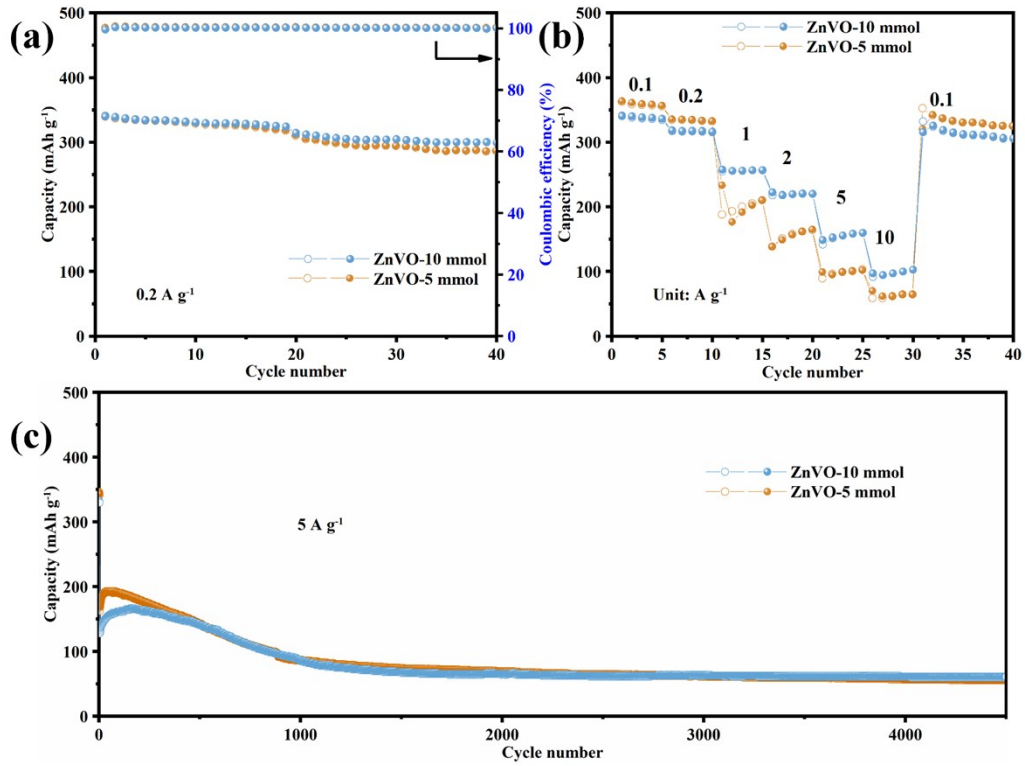

Fig. S14 a) Cycling performance at 0.2 A g^{-1}, b) rate performance, and c) long cycling performance at 5 A g^{-1} of ZnVO prepared at different Zn^{2+} concentration.

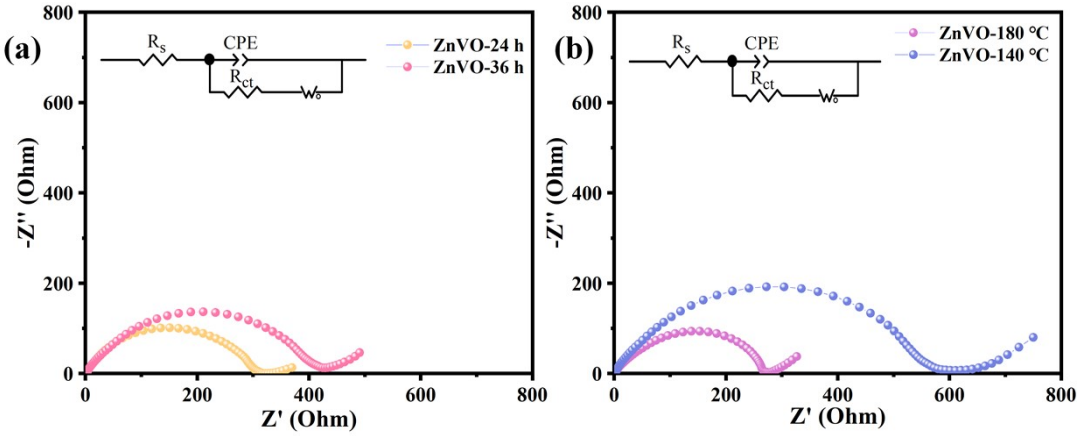

Fig. S15 Nyquist plots of ZnVO electrodes synthesized at a) different times and b) different temperatures.

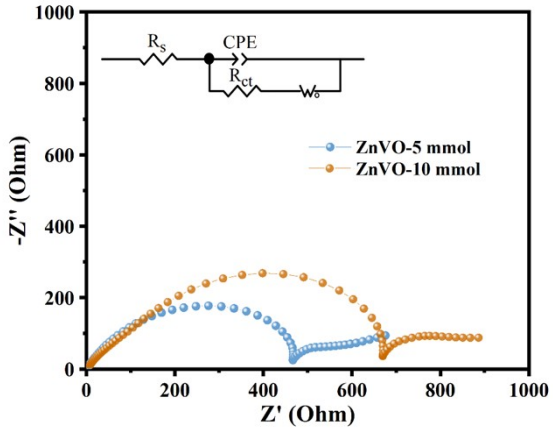

Fig. S16 Nyquist plots of ZnVO electrodes synthesized at different Zn^{2+} concentration.

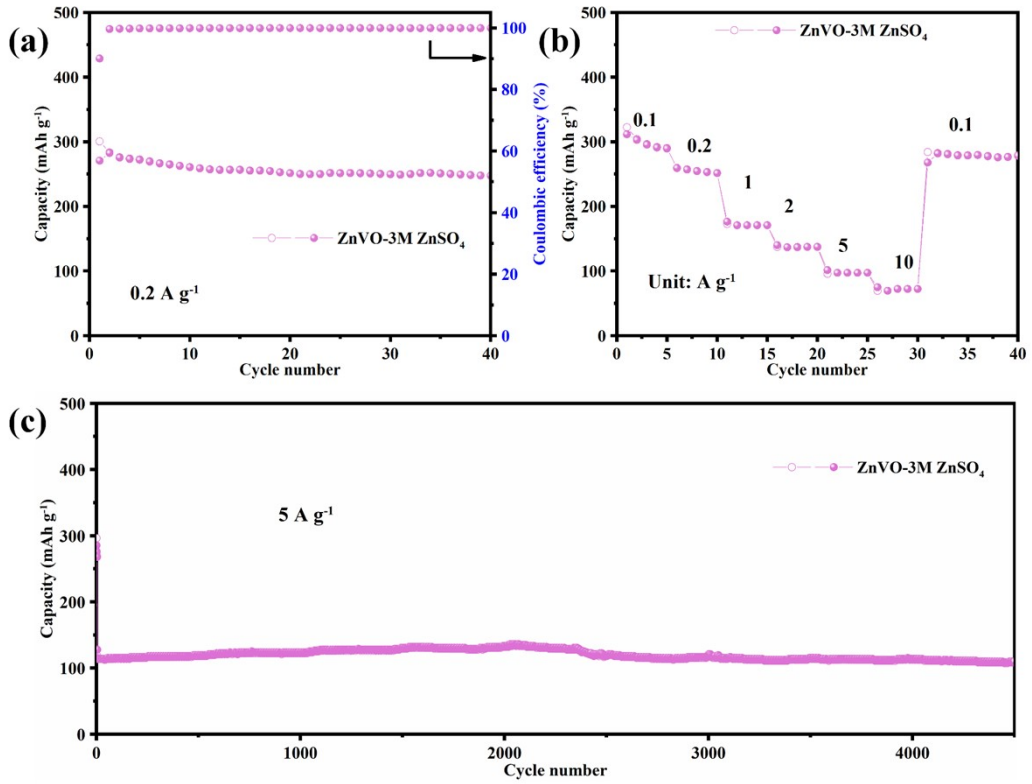

Fig. S17 a) Cycling performance at 0.2 A g^{-1}, b) rate performance, and c) long cycling performance at 5 A g^{-1} of ZnVO-160 ℃-30 h in 3M $ZnSO_4$ electrolytes.

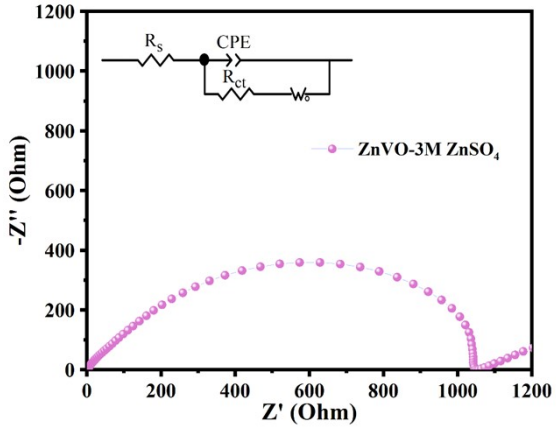

Fig. S18 Nyquist plots of ZnVO-160 ℃-30 h electrodes in 3M $ZnSO_4$ electrolytes.

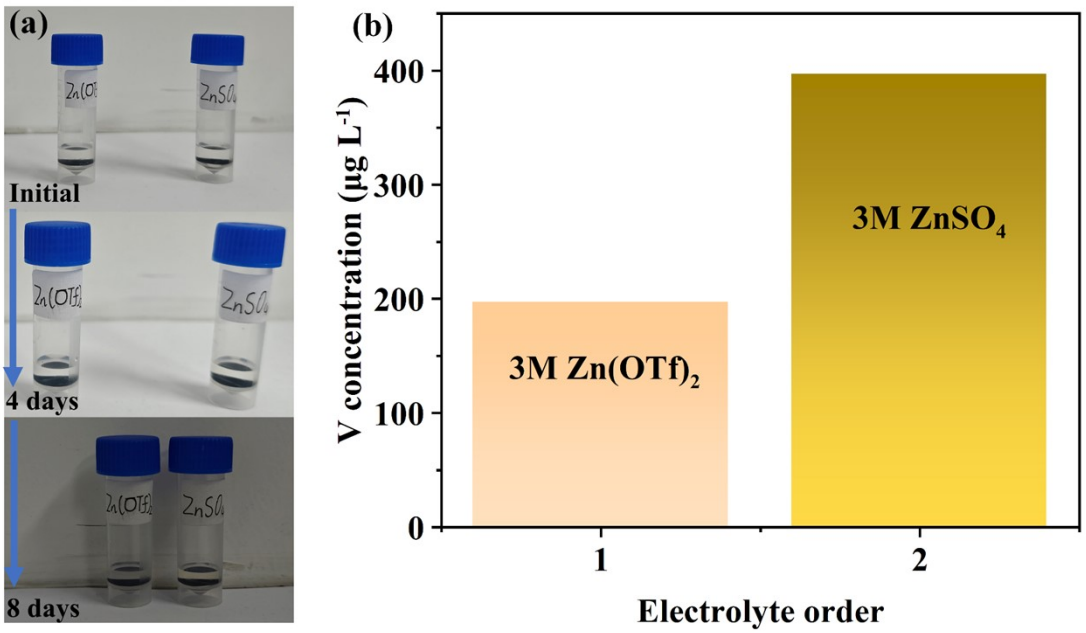

Fig. S19 a) The state changes of ZnVO electrodes in different electrolytes and b) the concentration of element V in different electrolytes after 8 days.

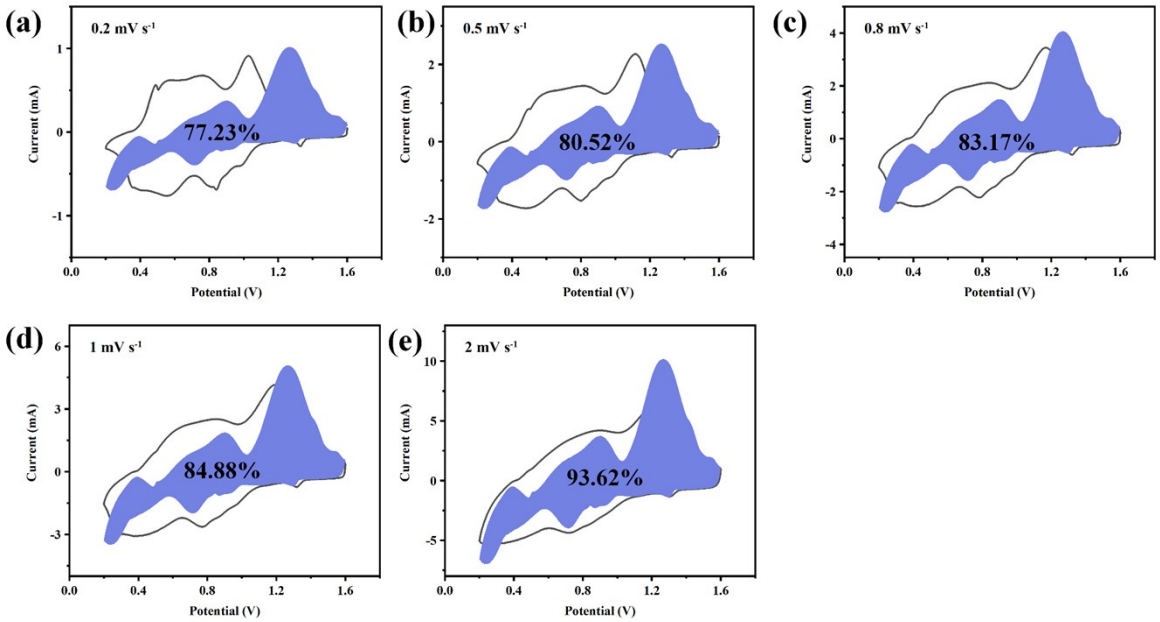

Fig. S20 The capacitive controlled portion of ZnVO at different scan rates.

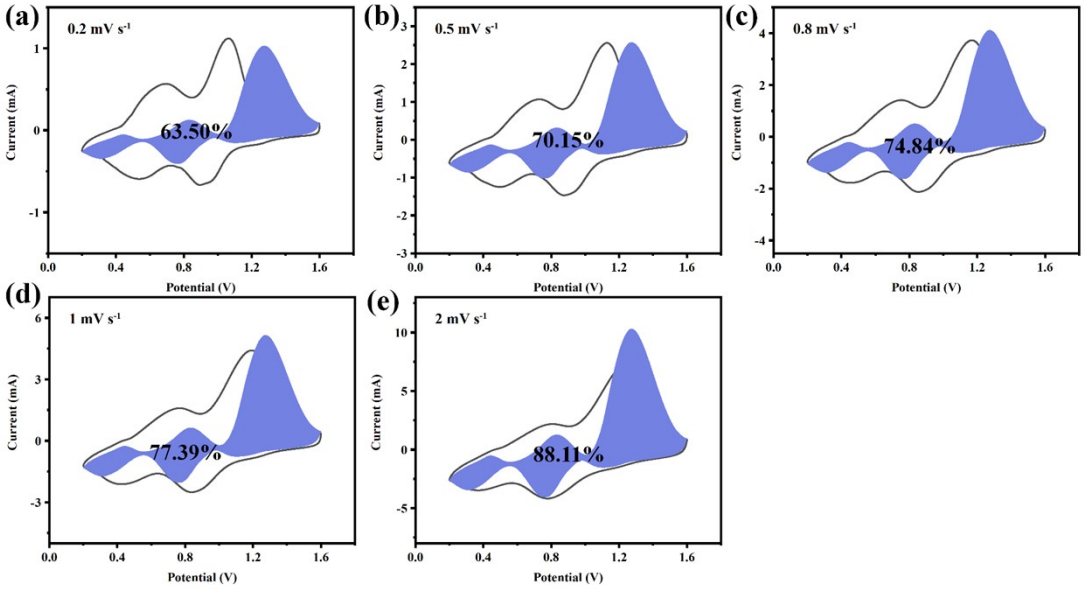

Fig. S21 The capacitive controlled portion of NiVO at different scan rates.

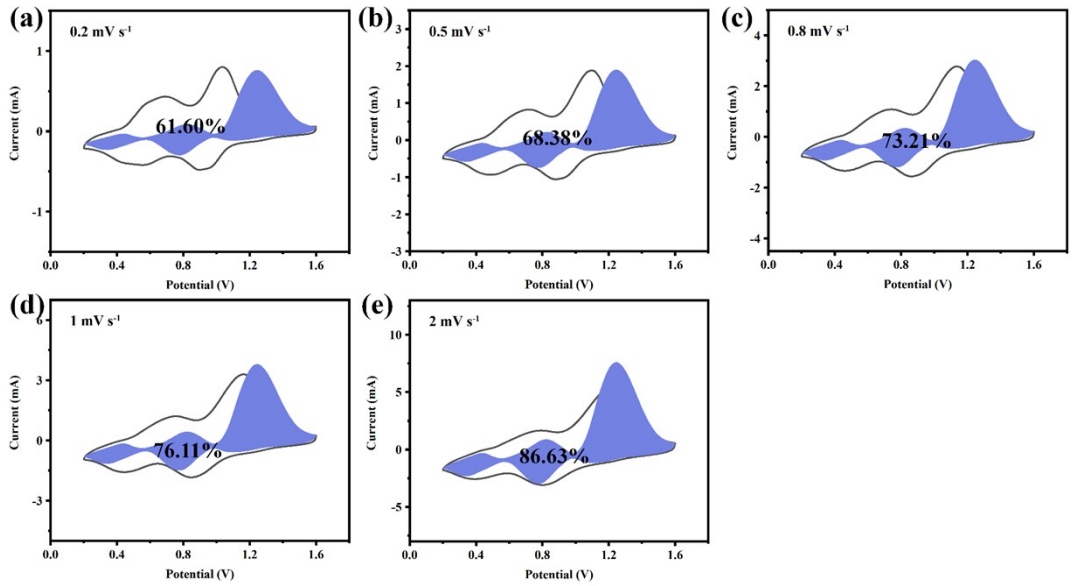

Fig. S22 The capacitive controlled portion of CoVO at different scan rates.

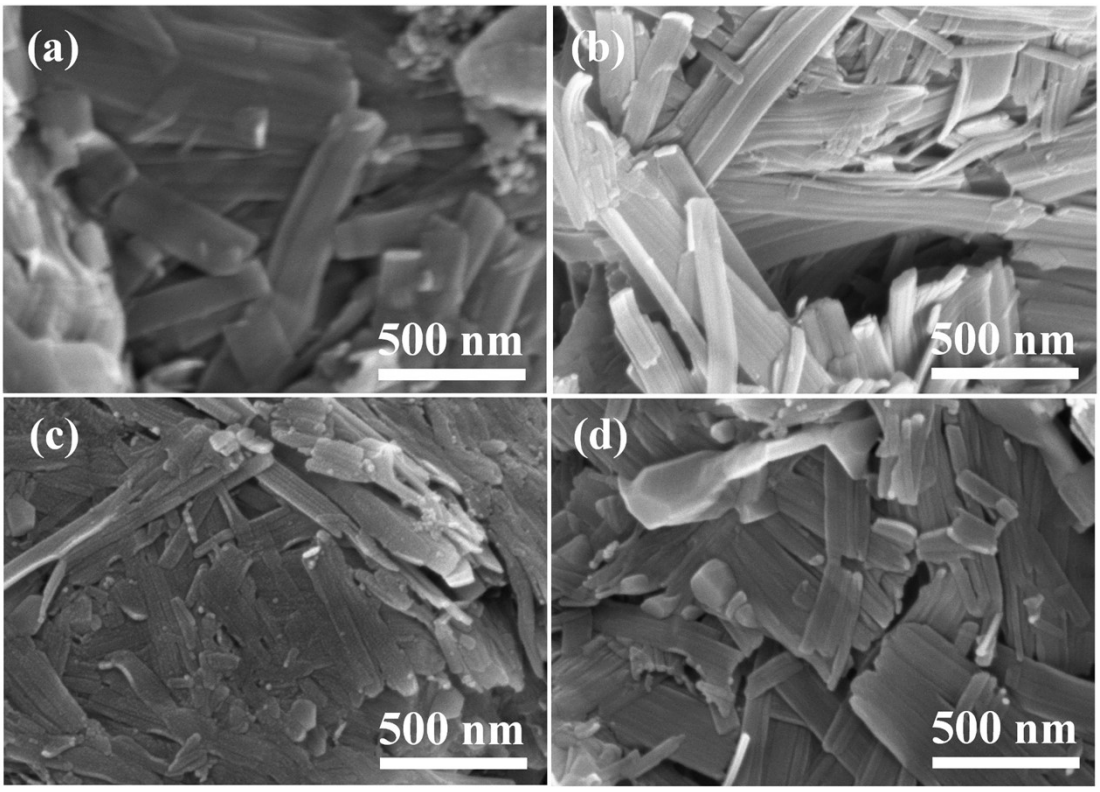

Fig. S23 SEM images of ZnVO electrodes for (a) the pristine state, (b) the 10th cycle, (c) the 20th cycle, and (d) the 40th cycle.

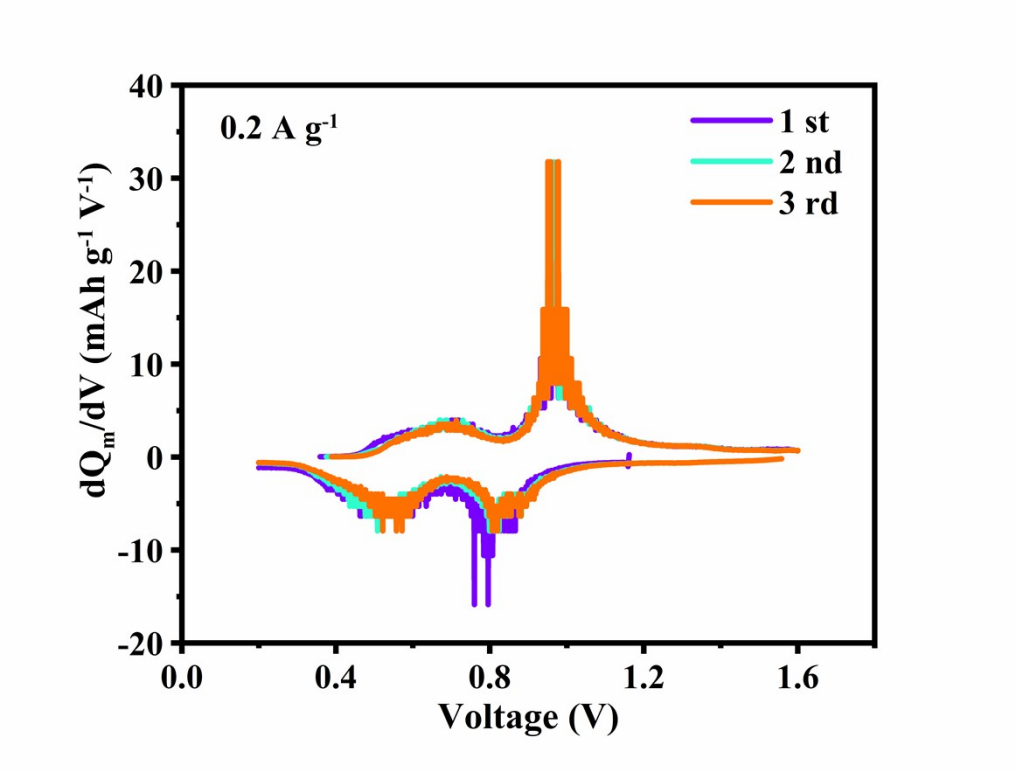

Fig. S24 The corresponding dQ_m/dV curves of flexible packaging battery at 0.2 A g^{-1}.

Table S1 Correlation between the size and charge of the pre-intercalated ion M (M = Zn, Co, Ni), and experimentally obtained structure (interlayer spacing) and composition (x in $M_xV_5O_{12}$) of the $M_xV_5O_{12}$ materials.

M in $M_xV_5O_{12}$	Ion radius(Å)	Hydrated ion radius (Å)	Interlayer spacing (Å)	x in $M_xV_5O_{12}$(EDS)	x in $M_xV_5O_{12}$ (ICP-MS)
Zn^{2+}	0.74	4.30	13.465	0.99	0.99
Co^{2+}	0.72	4.23	13.327	0.52	0.60
Ni^{2+}	0.70	4.04	13.193	0.63	0.58

Table S2 Performance comparison between ZnVO and recently reported vanadium-based materials.

Cathode	Specific capacity	Loss rate per cycle（cycles, current density）	Reference
$Zn_{0.99}V_5O_{12}\cdot 1.28H_2O$	416 mAh g^{-1} (0.1 A g^{-1})	0.000687% (15000, 5 A g^{-1})	This work
$Ca_{0.22}V_2O_5\cdot nH_2O$/rGO	409 mAh g^{-1} (0.05 A g^{-1})	0.005% (2000, 4 A g^{-1})	[2]
$Mg_{0.23}V_2O_5\cdot 1.0H_2O$	393 mAh g^{-1} (0.2 A g^{-1})	0.0007% (2000, 5 A g^{-1})	[3]
$Cu_xV_2O_5\cdot nH_2O$	379 mAh g^{-1} (0.5 A g^{-1})	0.007% (1000, 4 A g^{-1})	[4]
$(NH_4)_xV_2O_5\cdot nH_2O$	372 mAh g^{-1} (0.1 A g^{-1})	0.01% (2000, 5 A g^{-1})	[5]
$Ca_{0.23}V_2O_5\cdot 0.95H_2O$	355.2 mAh g^{-1} (0.2 A g^{-1})	0.00115% (2000, 5 A g^{-1})	[6]
$Mg_{0.34}V_2O_5\cdot 0.84H_2O$	353 mAh g^{-1} (0.1 A g^{-1})	0.0015% (2000, 5 A g^{-1})	[7]
$Na_2V_6O_{16}\cdot 1.63H_2O$	352 mAh g^{-1} (0.05 A g^{-1})	0.00166 % (6000, 5 A g^{-1})	[8]
$(NH_4)_2V_6O_{16}$	323.5 mAh g^{-1} (0.1 A g^{-1})	0.01085% (2000, 0.1 A g^{-1})	[9]
$Zn_xV_2O_5\cdot nH_2O$	304 mAh g^{-1} (0.5 A g^{-1})	0.02% (2000, 20 A g^{-1})	[10]
$Zn_{0.25}V_2O_5\cdot 0.85H_2O$	300 mAh g^{-1} (0.05 A g^{-1})	0.019% (1000, 2.4 A g^{-1})	[11]
$Ag_2V_4O_{11}$	200 mAh g^{-1} (0.3 A g^{-1})	0.4% (100, 1 A g^{-1})	[12]
$(NH_4)_2V_{10}O_{25}\cdot 8H_2O$	228.8 mAh g^{-1} (0.1 A g^{-1})	0.00198% (5000, 10 A g^{-1})	[13]

Table S3 Kinetics comparison between ZnVO and other reported ZVO-H_2O materials.

Cathode	Interlayer spacing of (001) plane (Å)	R_{ct} (Ω)	Capacitive contribution ratio	$D_{Zn^{2+}}$ value ($cm^2\ s^{-1}$)	Reference
$Zn_{0.99}V_5O_{12}\cdot 1.28H_2O$	13.465	222	77.2% (0.2 mV s^{-1}) 84.9% (1 mV s^{-1})	1.3×10^{-9}~2.1×10^{-10}	This work
$Zn_xV_2O_5\cdot nH_2O$	12.81	350	/	/	[10]
$Zn_{0.25}V_2O_5\cdot 0.85H_2O$	/	/	/	10^{-9}~10^{-10}	[11]
$Zn_3V_2O_7(OH)_2\cdot 2H_2O$	12.58	/	62% (0.3 mV s^{-1})	10^{-9}~10^{-10}	[14]
$Zn_2V_2O_7$	/	/	56% (1 mV s^{-1})	/	[15]
$Zn_3V_2O_7(OH)_2\cdot 2H_2O$	7.2	2800	51% (0.2 mV s^{-1})	10^{-10}~10^{-11}	[16]
ZnV_2O_4	/	450	50.8% (1 mV s^{-1})	7×10^{-10}	[17]
$Zn_3V_2O_8\cdot 1.85H_2O$	7.67	/	/	/	[18]
$Zn_{0.31}V_2O_5$	10.3	950	68.8% (1 mV s^{-1})	/	[19]
$Zn_{0.64}V_6O_{13}\cdot 1.62H_2O$	12.5	/	/	/	[20]

Table S4 Kinetics comparison between ZnVO and other reported unmodified vanadium oxide materials.

Cathode	Interlayer spacing of (001) plane (Å)	R_{ct} (Ω)	Capacitive contribution ratio	$D_{Zn^{2+}}$ value ($cm^2\ s^{-1}$)	Reference
$Zn_{0.99}V_5O_{12}\cdot 1.28H_2O$	13.465	222	84.88% (1 mV s^{-1})	1.3×10^{-9}~2.1×10^{-10}	This work
$V_5O_{12}\cdot 6H_2O$	11.8	150	50.5% (0.4 mV s^{-1})	10^{-10}~10^{-11}	[21]
$V_5O_{12}\cdot 2.7H_2O$	13	60.9	95% (1 mV s^{-1})	10^{-10}~10^{-15}	[22]
$V_5O_{12}\cdot 6H_2O$	11.8	/	20.5% (1 mV s^{-1})	/	[23]
$V_5O_{12}\cdot 6H_2O$	13.4	671	85% (1 mV s^{-1})	10^{-9}~10^{-11}	[24]
$V_5O_{12}\cdot 6H_2O$	12.3	30	83.3% (1 mV s^{-1})	10^{-11}~10^{-13}	[25]

References

1 Z. Yao, Q. Wu, K. Chen, J. Liu and C. Li, *Energy Environ. Sci.*, 2020, **13**, 3149–3163.

2 T. Hu, Z. Feng, Y. Zhang, Y. Liu, J. Sun, J. Zheng, H. Jiang, P. Wang, X. Dong and C. Meng, *Inorg. Chem. Fron.*, 2021, **8**, 79–89.

3 W. Xu, C. Liu, Q. Wu, W. Xie, W.-Y. Kim, S.-Y. Lee and J. Gwon, *J. Mater. Chem. A*, 2020, **8**, 18327–18337.

4 C. Liu, M. Tian, M. Wang, J. Zheng, S. Wang, M. Yan, Z. Wang, Z. Yin, J. Yang and G. Cao, *J. Mater. Chem. A*, 2020, **8**, 7713–7723.

5 L. Xu, Y. Zhang, J. Zheng, H. Jiang, T. Hu and C. Meng, *Mater. Today Energy*, 2020, **18**, 100509.

6 W. Zhou, M. Chen, A. Wang, A. Huang, J. Chen, X. Xu and C.-P. Wong, *J. Energy Chem.*, 2021, **52**, 377–384.

7 F. Ming, H. Liang, Y. Lei, S. Kandambeth, M. Eddaoudi and H. N. Alshareef, *ACS Energy Lett.*, 2018, **3**, 2602–2609.

8 P. Hu, T. Zhu, X. Wang, X. Wei, M. Yan, J. Li, W. Luo, W. Yang, W. Zhang, L. Zhou, Z. Zhou and L. Mai, *Nano Lett.*, 2018, **18**, 1758–1763.

9 L. Xu, Y. Zhang, H. Jiang, J. Zheng, X. Dong, T. Hu and C. Meng, *Colloids Surf. A Physicochem. Eng. Asp.*, 2020, **593**, 124621.

10 Y. Yang, Y. Tang, S. Liang, Z. Wu, G. Fang, X. Cao, C. Wang, T. Lin, A. Pan and J. Zhou, *Nano Energy*, 2019, **61**, 617–625.

11 D. Kundu, B. D. Adams, V. Duffort, S. H. Vajargah and L. F. Nazar, *Nat. Energy*, 2016, **1**, 16119.

12 S. Guo, G. Fang, S. Liang, M. Chen, X. Wu and J. Zhou, *Acta Mater.*, 2019, **180**, 51–59.

13 T. Wei, Q. Li, G. Yang and C. Wang, *J. Mater. Chem. A*, 2018, **6**, 20402–20410.

14 C. Xia, J. Guo, Y. Lei, H. Liang, C. Zhao and H. N. Alshareef, *Adv. Mater.*, 2018, **30**, 1705580.

15 B. Sambandam, V. Soundharrajan, S. Kim, M. H. Alfaruqi, J. Jo, S. Kim, V. Mathew, Y. Sun and J. Kim, *J. Mater. Chem. A*, 2018, **6**, 3850–3856.

16 H. Cao, C. Peng, Z. Zheng, Z. Lan, Q. Pan, U. G. Nielsen, P. Norby, X. Xiao and S. Mossin, *Electrochim. Acta*, 2021, **388**, 138646.

17 Y. Liu, C. Li, J. Xu, M. Ou, C. Fang, S. Sun, Y. Qiu, J. Peng, G. Lu, Q. Li, J. Han and Y. Huang, *Nano Energy*, 2020, **67**, 104211.

18 Z. Xie, J. Lai, X. Zhu and Y. Wang, *ACS Appl. Energy Mater.*, 2018, **1**, 6401–6408.

19 Z. Pang, B. Ding, J. Wang, Y. Wang, L. Xu, L. Zhou, X. Jiang, X. Yan, J. P. Hill, L. Yu and Y. Yamauchi, *Chem. Eng. J.*, 2022, **446**, 136861.

20 T. Lv, G. Zhu, S. Dong, Q. Kong, Y. Peng, S. Jiang, G. Zhang, Z. Yang, S. Yang, X. Dong, H. Pang and Y. Zhang, *Angew. Chem. Int. Ed.*, 2023, **135**, e202216089.

21 N. Zhang, M. Jia, Y. Dong, Y. Wang, J. Xu, Y. Liu, L. Jiao and F. Cheng, *Adv. Funct. Mater.*, 2019, **29**, 1807331.

22 C.-E. M. Lewis, J. F. S. Fernando, D. P. Siriwardena, K. L. Firestein, C. Zhang and D. V. Golberg, *ACS Appl. Energy Mater.*, 2022, **5**, 4159–4169.

23 P. Yadav, N. Sanna Kotrappanavar, P. B. Naik, H. K. Beere, K. Samanta, N. S. Reddy, J. S. Algethami, M. Jalalah, F. A. Harraz and D. Ghosh, *ACS Appl. Energy Mater.*, 2023, **6**, 1799–1809.
24 T. Wei, Q. Li, G. Yang and C. Wang, *Adv. Energy Mater.*, 2019, **9**, 1901480.
25 B. Xiao, J. Chen, C. Hu, L. Mou, W. Yang, W. He, Z. Lu, S. Peng and J. Huang, *Adv. Funct. Mater.*, 2023, **33**, 2211679.